Correlating the structure and localized surface plasmon resonance of single silver right bipyramids

2012 Nanotechnology 23 444005

(http://iopscience.iop.org/0957-4484/23/44/444005)

Nanotechnology **23** (2012) 444005 (6pp) doi:10.1088/0957-4484/23/44/444005

Correlating the structure and localized surface plasmon resonance of single silver right bipyramids

Emilie Ringe[1], Jian Zhang[1], Mark R Langille[1], Chad A Mirkin[1,2], Laurence D Marks[2] and Richard P Van Duyne[1]

[1] Department of Chemistry, Northwestern University, 2145 Sheridan Road, Evanston, IL 60208, USA
[2] Department of Materials Science and Engineering, Northwestern University, 2220 Campus Drive, Evanston, IL 60208, USA

E-mail: emilieringe@u.northwestern.edu

Received 7 February 2012, in final form 30 March 2012
Published 18 October 2012
Online at stacks.iop.org/Nano/23/444005

Abstract
Localized surface plasmon resonances (LSPRs), collective electron oscillations in metal nanoparticles, are being heavily scrutinized for applications in prototype devices and circuits, as well as for chemical and biological sensing. Both the plasmon frequency and linewidth of a LSPR are critical factors for application optimization, for which their dependence on structural factors has been qualitatively unraveled over the past decade. However, quantitative knowledge based on systematic single particle studies has only recently become available for a few particle shapes. We show here that to understand the effect of structure (both size and shape) on plasmonic properties, one must take multiple parameters into account. We have successfully done so for a large data set on silver right bipyramids. By correlating plasmon energy and linewidth with edge length and corner rounding for individual bipyramids, we have found that the corner rounding has a significant effect on the plasmon energy for particles of the same size, and thus corner rounding must be taken into account to accurately describe the dependence of a LSPR on nanoparticle size. A detailed explanation of the phenomena responsible for the observed effects and their relationship to each other is presented.

S Online supplementary data available from stacks.iop.org/Nano/23/444005/mmedia

(Some figures may appear in colour only in the online journal)

1. Introduction

Metal nanoparticles are attracting much attention in the scientific community because, unlike bulk materials, their properties can be tuned based on their shape and size. In particular, the localized surface plasmon resonance (LSPR) properties of noble metal (Ag and Au, for example) particles have shown promise for use in information [1–5] and sensing [6–11] applications. The enhanced electromagnetic fields around a particle due to LSPR excitation have been used for surface-enhanced Raman spectroscopy (SERS) [12–14], while the resulting optical properties of such particles make them attractive for a variety of chemical [15–18] and biological detection schemes [11, 19–24], some of which have been commercialized and FDA-cleared. In addition, they exhibit bright, environment-dependent light scattering and absorption, leading to their use as nanoscale refractive index sensors [6, 19, 25–27]. Much effort has been devoted to understanding the factors influencing the LSPR energy and its sensitivity to the surrounding environment, from early bulk measurements on particle arrays to more recent single particle studies [28–34].

A successful approach that has been used to unravel structure–plasmonic activity relationships is to perform correlated single particle spectroscopy and electron microscopy: this surmounts the difficulties associated with the typically large structural inhomogeneities derived from chemical particle synthesis. The development of methods for synthe-

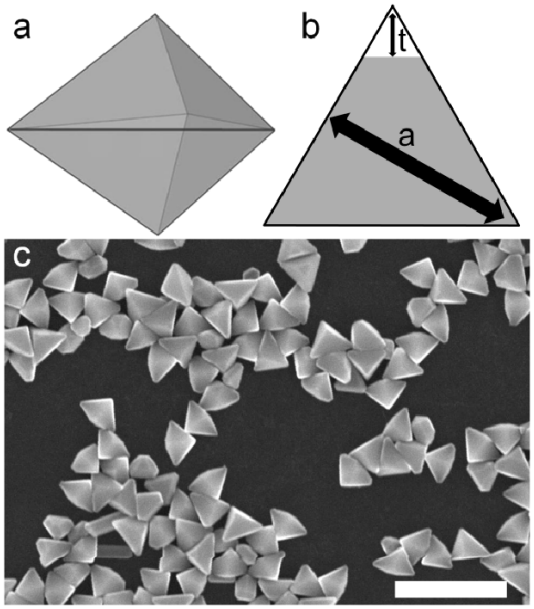

Figure 1. Particle geometry and definition of structural parameters. (a) 3D model of a right bipyramid, (b) structural parameters: truncation length (t) and height of the equilateral base (a) (c) micrograph of a typical reaction mixture obtained on a Hitachi S4800-II scanning electron microscope. The scale bar in (c) is 500 nm.

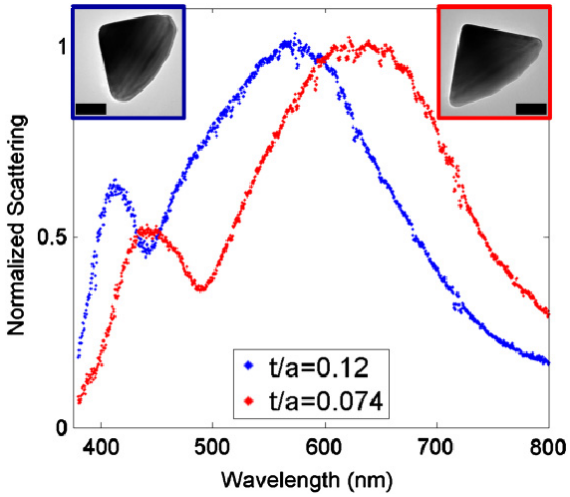

Figure 2. Effect of equatorial corner rounding on the LSPR spectrum of a bipyramid. Blue curve, left inset: round particle ($t/a = 0.12$). Red curve, right inset: sharp particle ($t/a = 0.074$). The scale bars are 50 nm.

sizing well-characterized silver nanostructures of well-defined shapes, [35–40] in addition to early spectroscopic studies on colloidal silver particles, [32] paved the road for more recent systematic, statistics-based analyses published on decahedra [30], cubes [31], cages [41], spheroids [34], and flat nanoprisms [3, 33, 42]. We have previously noted [43] that the size dependences of very rounded and sharp bipyramids were significantly different. Since this early analysis we have acquired more data on correlated plasmonic (peak position and width) and structural (size and corner truncation) properties. In this paper, we demonstrate that the relationship between plasmonic properties and particle shape for silver right triangular bipyramids [43–45] is more accurately described by including multiple structural parameters, namely particle size and corner rounding, in the quantification of particle shape. These results reveal the effects of individual parameters, as well as their interplay, on the plasmonic properties of individual metal nanoparticles.

2. Experimental methods

Silver right bipyramids were synthesized using a previously published plasmon-mediated technique [44]. An aqueous suspension of particles was deposited and dried on the Formvar (polyvinyl formal, refractive index = 1.5 [46]) side of carbon type B grids obtained from Ted Pella, Inc. Dark-field scattering, performed with unpolarized light, was used to obtain LSPR, following a previously reported procedure [29, 31, 47], summarized in figure S1 (available at stacks.iop.org/Nano/23/444005/mmedia). Spectra of 123 individual silver bipyramids were fit to obtain peak positions and widths. Transmission electron microscope (TEM) images providing nm-resolution structural information were obtained using a JEOL JEM2100 FAST TEM operated at 200 kV. In order to minimize oxidation, TEM was performed within two days of the optical characterization. Bipyramid size is defined as the height of the equilateral triangle base (a) measured from an untruncated bipyramid, while the truncation, t, is the height of a triangle fitting in the empty corner of the equilateral base defined by the perfect bipyramid overlay (figures 1 and S2 available at stacks.iop.org/Nano/23/444005/mmedia). The complete data set used is reported in table S1 (available at stacks.iop.org/Nano/23/444005/mmedia). The error associated with the structural parameters is approximately ± 1 nm. Relative corner rounding, a size-independent parameter, was computed as t/a.

3. Results and discussion

Silver right triangular bipyramids were prepared using a plasmon-mediated synthesis [44]. This method, which has also been used to produce nanostructures such as triangular nanoprisms [35, 37] and rods [48, 49], is advantageous for these studies because the size of the bipyramids can be controlled by the excitation wavelength, allowing bipyramids of different sizes to be readily prepared [44]. The right triangular bipyramids are a {111} twinned structure with six equivalent triangular {100} faces and an equilateral triangular base [45], as can be seen in the scanning electron micrograph and model presented in figure 1. Typical bipyramid spectra and TEM images are presented in figure 2. The shape and position of the plasmon peaks, obtained from dark-field microscopy with unpolarized light, are in excellent agreement with previous calculations [44]. The peak around 420 nm can be attributed, on the basis of computational results [44], to the transverse dipolar resonance (oscillation perpendicular to the equilateral triangle base), while the lower energy peak

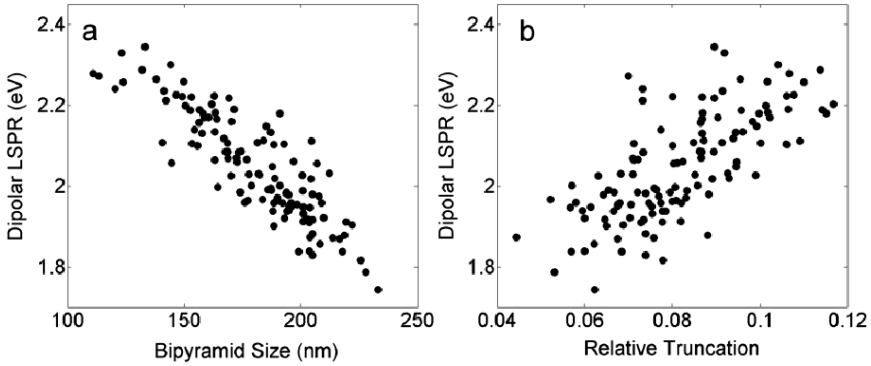

Figure 3. Single parameter effects on the longitudinal dipolar resonance energy of Ag bipyramids, showing the inadequacy of either parameter to truly describe the variation. (a) Effect of size, (b) effect of corner rounding.

around 600 nm arises from the longitudinal dipolar resonance (oscillation parallel to the triangular base).

3.1. Single parameter effects

From the TEM images, the size of the bipyramids and the truncation of the equatorial tips (i.e. those on the corner of the equilateral {111} twin plane, as defined in figure 1) were obtained. Their effect on the longitudinal dipolar plasmon resonance can be seen in figure 3. A shift to lower energy is observed for increasing size (figure 3(a)), while a shift to higher energy is seen for larger corner rounding (figure 3(b)). This work indeed confirms and expands on previous calculations which demonstrate the sensitivity of the longitudinal peak to size and rounding of the equatorial corners [44].

Explanations for the effect of size and shape shown in figure 3 can be found in moderately straightforward models developed decades ago. The simplest model of localized plasmon resonance frequency is the electrostatic limit of Mie theory, [50] in which the speed of light is considered infinite and thus all parts of the particle are subject to the same field. For a particle with a dielectric constant $\varepsilon_{(\lambda)} = \varepsilon_{r(\lambda)} + i\varepsilon_{i(\lambda)}$ in a homogeneous medium described by ε_m, the extinction efficiency $Q_{ext(\lambda)}$ of an ellipsoid with the electric field of the incoming radiation parallel to its main axis is obtained by the so-called Mie–Gans [51] theory:

$$Q_{ext(\lambda)} = \frac{2\pi V \varepsilon_m^{3/2}}{GL^2\lambda} \frac{\varepsilon_i}{[\varepsilon_T + (\frac{1-L}{L})\varepsilon_m]^2 + \varepsilon_L^2} \qquad (1)$$

where V is the volume of the particle, G is its projected cross-sectional area, and L is a geometric factor. Analytical solutions of L are available for spheres ($L = 1/3$), and prolate ($L < 1/3$) and oblate ($L > 1/3$) ellipsoids [52]. This equation qualitatively describes the plasmon energy dependence on shape; for example, the energy decreases for increasing aspect ratio in particles such as rods approximated as prolate ellipsoids. The lack of analytical solutions for L prevents us from making definitive statements, but the Mie–Gans equation nevertheless predicts the observed trend (figure 3(b)) that as particles become closer to spheres, their plasmon energy increases. We note that this is not a volume effect, as the volume difference between sharp and rounded bipyramids is a few per cent at most, and not enough to be responsible for the significant shift observed.

Despite being adequate to describe shape effects, the electrostatic limit embodied in the Mie–Gans equation does not properly model the size dependence of the plasmon frequency observed in this work or that of others [30, 31, 53], for particles as small as $0.1\lambda_m$, ($\lambda_m = \lambda/\sqrt{\varepsilon_m}$) [54]. Retardation effects, due to the finite speed of light, must thus be included. They explain the redshift of the plasmon with size increase in relatively simple and intuitive terms: the plasmon resonance frequency changes with dimension because the electron oscillation has to accommodate the difference in electromagnetic phase between one end of the particle and the other. In other words, the plasmon frequency is inversely proportional to the distance between poles of charges, such that a particle with long dimensions along the electron oscillation will have a lower LSPR frequency (longer wavelength) than a short particle. Retardation effects can be analytically modeled for spheres, and yield very accurate results for diameters up to 150 nm [54], while numerical methods have to be used for more complex shapes. Such effects allow us to understand and explain the trends observed in figure 3(a).

3.2. Two parameter fits: size and truncation

While the correlation observed between size, corner rounding and longitudinal plasmon resonance frequency presented in figure 3 can rather convincingly be stated on the basis of the 123 data points analyzed, a significant amount of 'noise' remains present when trying to relate the plasmon frequency to either of the structural parameters. A very basic way to assess if a single parameter is sufficient to fit a data set is the *R*-square value. While *R*-square is not a measure of error, it is a useful number in that it assesses what fraction of the variation in the data set is due to the parameter(s) used in the fit. Thus a *R*-square of 1 (or 100%) means that there are no other parameters to consider, and a *R*-square of 0 means that this parameter has no effect on the results. Going back to figure 3 and its 'noise', it is not surprising to find relatively low values of *R*-square: 75% for the size effect (figure 3(a)),

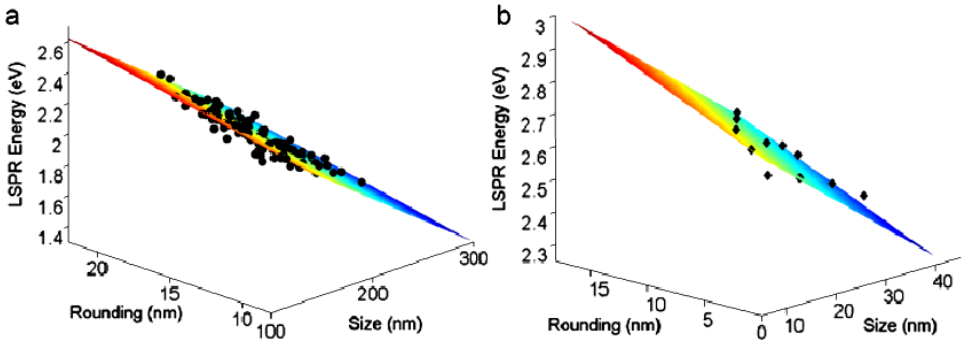

Figure 4. Effect of size and corner rounding on the longitudinal dipolar resonances of nanoparticles. (a) Experimental data on Ag bipyramids (fit described by equation (2)), (b) Ag nanorods based on calculations from Prescott and Mulvaney [57] (fit described by equation S5 available at stacks.iop.org/Nano/23/444005/mmedia).

and 49% for the truncation effect (figure 3(b)). This clearly indicates that neither parameter alone is sufficient to describe the variation in plasmon energy.

Given the large number of experimental data points, it was possible to fit a two-parameter equation (using non-linear least squares), expressing the longitudinal plasmon resonance energy as a function of both size and corner rounding. The following form, which provides the good fit to the data seen in figure 4, was chosen:

$$\mathrm{LSPR}_{(\mathrm{eV})} = -0.0051(0.0003)a_{(\mathrm{nm})} + 0.019(0.003)t_{(\mathrm{nm})} + 2.69(0.06). \quad (2)$$

The tight 95% confidence bounds on the fit coefficients (in parenthesis) indicate the low errors associated with the model, while the *R*-square value of 0.88 signifies that the fit based on both size and corner rounding (figure 4) explains 88% of the variation in the experimental data. Clearly, size and corner rounding comprehensively dictate the position of the plasmon resonance frequency, and the latter does influence the plasmon size dependence, as noted previously [43]. The remaining noise in figure 4 can be attributed to variation in the transverse corner truncation; calculations have shown that the geometry of these tips can slightly affect the longitudinal plasmon [44], and was not accounted for in this study because of the experimental difficulties associated with obtaining accurate structural information on the transverse tips. Because this three-dimensional statistical analysis very effectively describes the optical properties of single right bipyramids, we will explain the phenomena responsible for the observed trends, beyond the simple 1-parameter arguments presented above. Note that recently the optical properties of colloidal core–shell Ag–Ag_2O particles have also been fit to a three-dimensional plot, although in those reports the two structural parameters used were the core radius and shell thickness of the particles [55, 56], whereas here we have related the optical properties of the bipyramids to their size and corner rounding.

The work of Prescott and Mulvaney [57], which summarizes the effect of size, aspect ratio, and corner rounding on Au nanorods modeled as ellipsoidally capped cylinders, is useful in understanding the current results. They used the discrete dipole approximation (DDA) to calculate effective geometric factors L_{eff}, which include retardation effects, to be used in Mie–Gans theory. This approach accurately yields a redshift due to increased size and elongation, and a blueshift due to increased corner rounding. We have used these geometric factors for rods of aspect ratio of 2, together with the dielectric constant of Ag from Johnson and Christy [58], to calculate the peak energies for the 12 data points in figure 4(b), table S2, and figure S4 (available at stacks.iop.org/Nano/23/444005/mmedia).

The similarity between the experimental and calculated data in figure 4 confirms the trends observed and helps explain them. A smaller decrease of the plasmon resonance energy with size for more rounded particles can also be noted in the numerical data presented by Slaughter *et al* [59] and Bryant *et al* [60], yet neither discussed this feature. This multi-parameter effect on the size dependence of the plasmon energy can be understood from a simple geometric argument. For bipyramids of edge length *a* and truncation *t*, the tip-to-edge distance (real height) is *a*–*t*, i.e. smaller for more rounded particles. Retardation effects (phase differences between the particle tips) are responsible for the size dependence of plasmon frequency. Retardation is less present in a more round particle because of the shorter real height, explaining the blueshift observed with increased truncation. Additionally, as *a* is doubled, the idealized height is also doubled, but the true (truncated, *a*–*t*) distance is not: the absolute increase is smaller for more rounded bipyramids. However, if this effect was solely responsible for the observed trend, the coefficient of *t* in equation (2) would be equal in magnitude and opposite in sign to the coefficient of *a*, i.e. a fit relating the plasmon energy to the truncated height (*a*–*t*) would be best. Clearly, variations in tip sharpness also change the charge distribution, such that for rounded particles opposite charges become even closer than from this geometrical argument alone. The phase difference between the tips and the charge distribution not changing equivalently thus leads to a dissimilar increase in retardation for the same (idealized) size increase in rounded and sharp particles. Consequently, the plasmon frequency of rounded particles is less dependent on size than that of sharp particles, as experimentally observed. Comparing to the Prescott and Mulvaney [57] data on Ag (figure 4(b)) and Au (figure S4 and

table S2 available at stacks.iop.org/Nano/23/444005/mmedia) rods, where the rounding is defined in a way which retains the distance between the tips' ends, one can argue that the distance between the center of charge density varies, being shorter for more rounded particles. We believe the same explanation applies to the influence of aspect ratio on the slope of the size-dependent plasmon frequency, as noticed in the calculation of Bryant *et al* [60].

3.3. Effect of size and truncation on FWHM

We have also attempted to model the plasmon linewidth of bipyramids as a function of size and shape, and found that size is the only factor having a statistically significant contribution. The linear correlation between a and the linewidth of the longitudinal plasmon is presented in figure S3 and equation S4 (available at stacks.iop.org/Nano/23/444005/mmedia). In this case the R-square value is only 33%, indicating that other effects may be important. Small changes in the dielectric environment, surface oxidation, transverse tip truncation, and the possible appearance of higher order modes (not included in the peak fitting) can indeed affect plasmon decay, thus influencing the results obtained.

4. Conclusion

The complex behavior of nanoparticles makes them potentially valuable for many applications, given that we can understand and predict their useful properties. This paper has demonstrated and explained that optical properties are best described by a combination of factors for heavily rounded particles. In this specific case, size and shape not only affect the plasmon resonance frequency of silver bipyramids but also contribute to the effect of the other parameter, i.e. they are intertwined. Such results will play a crucial role in the design of future plasmonic devices.

Acknowledgments

This work was supported by the DoD, AFOSR/DARPA Project BAA07-61, AFOSR FA9550-08-1-0221, NSF (CHE0911145), NSF-NSEC (EEC-0647560), NSF-NERC and the NSF MRSEC (DMR-1121262) at the Materials Research Center of Northwestern University. CAM is grateful for support by AFOSR Award FA9550-09-1-0294, DoD/NSSEFF/NPS Award N00244-09-1-0012, Non-equilibrium Energy Research Center (NERC) DOE Award DE-SC0000989, Nanoscale Science and Engineering Initiative NSF Award EEC-0647560, NSF MRSEC (DMR-0520513) and CEMRI (DMR-1121262) and shared facilities at the Materials Research Center. Microscopy work was performed in the EPIC facility of the NUANCE Center which is supported by NSF-NSEC, NSF-MRSEC, Keck Foundation, the State of IL and NU. Any opinions, findings and conclusions or recommendations expressed in this publication are those of the authors and do not necessarily reflect the views of the agency sponsors.

References

[1] Ozbay E 2006 *Science* **311** 189–93
[2] Ebbesen T W, Genet C and Bozhevolnyi S I 2008 *Phys. Today* **61** 44–50
[3] Blaber M G, Henry A-I, Bingham J M, Schatz G C and Van Duyne R P 2012 *J. Phys. Chem.* C **116** 393–403
[4] Dionne J A, Sweatlock L A, Atwater H A and Polman A 2006 *Phys. Rev.* B **73** 035407
[5] Bechtel J H, Smith W L and Bloembergen N 1977 *Phys. Rev.* B **15** 4557–63
[6] Lee K-S and El-Sayed M A 2006 *J. Phys. Chem.* B **110** 19220–5
[7] Galush W J, Shelby S A, Mulvihill M J, Tao A, Yang P and Groves J T 2009 *Nano Lett.* **9** 2077–82
[8] Elghanian R, Storhoff J J, Mucic R C, Letsinger R L and Mirkin C A 1997 *Science* **277** 1078–81
[9] Haes A J, Chang L, Klein W L and Van Duyne R P 2005 *J. Am. Chem. Soc.* **127** 2264–71
[10] Burgin J, Liu M and Guyot-Sionnest P 2008 *J. Phys. Chem.* C **112** 19279–82
[11] Anker J N, Hall W P, Lyandres O, Shah N C, Zhao J and Van Duyne R P 2008 *Nature Mater.* **7** 442–53
[12] Stiles P L, Dieringer J A, Shah N C and Van Duyne R P 2008 *Ann. Rev. Anal. Chem.* **1** 601–26
[13] Kneipp K, Kneipp H, Itzkan I, Dasari R R and Feld M S 2002 *J. Phys.: Condens. Matter* **14** R597–624
[14] Brus L 2008 *Acc. Chem. Res.* **41** 1742–29
[15] Rex M, Hernandez F E and Campiglia A D 2006 *Anal. Chem.* **78** 445–51
[16] Forzani E S, Foley K, Westerhoff P and Tao N 2007 *Sensors Actuators* B **123** 82–8
[17] Lee J S and Mirkin C A 2008 *Anal. Chem.* **80** 6805–8
[18] Lee J S and Mirkin C A 2007 *Angew. Chem. Int. Edn* **46** 4093–6
[19] Mayer K M and Hafner J H 2011 *Chem. Rev.* **111** 3828–57
[20] Haes A J and Van Duyne R P 2002 *J. Am. Chem. Soc.* **124** 10596–604
[21] Sepúlveda B, Angelomé P C, Lechuga L M and Liz-Marzán L M 2009 *Nano Today* **4** 244–51
[22] Taton T A, Mirkin C A and Letsinger R L 2000 *Science* **289** 1757–60
[23] Hall W P, Ngatia S N and Duyne R P V 2011 *J. Phys. Chem.* C **115** 1410–4
[24] Huang H, Liu X, Liao B and Chu P K 2011 *Plasmonics* **6** 1–9
[25] Willets K A and Van Duyne R P 2007 *Ann. Rev. Phys. Chem.* **58** 267–97
[26] Wang Y, Qian W, Tan Y and Ding S 2008 *Biosens. Bioelectron.* **23** 1166–70
[27] Chen H, Kou X, Yang Z, Ni W and Wang J 2008 *Langmuir* **24** 5233–7
[28] Jensen T R, Malinsky M D, Haynes C L and Van Duyne R P 2000 *J. Phys. Chem.* B **104** 10549–56
[29] McMahon J M, Wang Y, Sherry L J, Van Duyne R P, Marks L D, Gray S K and Schatz G C 2009 *J. Phys. Chem.* C **113** 2731–5
[30] Rodríguez-Fernández J, Novo C, Myroshnychenko V, Funston A M, Sánchez-Iglesias A, Pastoriza-Santos I, Pérez-Juste J, García de Abajo F J, Liz-Marzán L M and Mulvaney P 2009 *J. Phys. Chem.* C **113** 18623–31
[31] Ringe E, McMahon J M, Sohn K, Cobley C M, Xia Y, Huang J, Schatz G C, Marks L D and Van Duyne R P 2010 *J. Phys. Chem.* C **114** 12511–6
[32] Mock J J, Barbic M, Smith D R, Schultz D A and Schultz S 2002 *J. Chem. Phys.* **116** 6755–9
[33] Munechika K, Smith J M, Chen Y and Ginger D S 2007 *J. Phys. Chem.* C **111** 18906–11
[34] Tcherniak A, Ha J W, Dominguez-Medina S, Slaughter L S and Link S 2010 *Nano Lett.* **10** 1398–404

[35] Jin R, Cao Y C, Hao E, Métraux G S, Schatz G C and Mirkin C A 2003 *Nature* **425** 487–90
[36] Sun Y and Xia Y 2002 *Science* **298** 2176–9
[37] Jin R, Cao Y, Mirkin C A, Kelly K L, Schatz G C and Zheng J 2001 *Science* **294** 1901–3
[38] Jana N R, Gearheart L and Murphy C J 2001 *J. Phys. Chem.* B **105** 4065–7
[39] Sau T K and Murphy C J 2004 *J. Am. Chem. Soc.* **126** 8648–9
[40] Nikoobakht B and El-Sayed M A 2003 *Chem. Mater.* **15** 1957–62
[41] Hu M, Chen J, Marquez M, Xia Y and Hartland G V 2007 *J. Phys. Chem.* C **111** 12558–65
[42] Nelayah J, Kociak M, Stéphan O, Geuquet N, Henrard L, García de Abajo F J, Pastoriza-Santos I, Liz-Marzán L M and Colliex C 2010 *Nano Lett.* **10** 902–7
[43] Ringe E *et al* 2010 *Mater. Res. Soc. Symp. Proc.* **1208** O10–02
[44] Zhang J, Li S, Wu J, Schatz G C and Mirkin C A 2009 *Angew. Chem. Int. Edn* **48** 7787–91
[45] Zhang J, Langille M R and Mirkin C A 2010 *J. Am. Chem. Soc.* **132** 12502–10
[46] Shukla R P, Chowdhury A and Gupta P D 1994 *Opt. Eng.* **33** 1881–4
[47] Wang Y, Eswaramoorthy S K, Sherry L J, Dieringer J A, Cadmen J P, Schatz G C, Van Duyne R P and Marks L D 2009 *Ultramicroscopy* **109** 1110–3
[48] Langille M R, Zhang J and Mirkin C A 2011 *Angew. Chem. Int. Edn* **50** 3543–7
[49] Zhang J, Langille M R and Mirkin C A 2011 *Nano Lett.* **11** 2495–8
[50] Mie G 1908 *Ann. Phys.* **25** 377–445
[51] Gans R 1912 *Ann. Phys.* **342** 881–900
[52] Bohren C F and Huffman D R 1983 *Absorption and Scattering of Light by Small Particles* (New York: Wiley)
[53] Link S and El-Sayed M A 1999 *J. Phys. Chem.* B **103** 4212–7
[54] Myroshnychenko V, Rodríguez-Fernandez J, Pastoriza-Santos I, Funston A M, Novo C, Mulvaney P, Liz-Marzán L M and García de Abajo F J 2008 *Chem. Soc. Rev.* **37** 1792–805
[55] Santillán J M J, Scaffardi L B and Schinca D C 2011 *J. Phys. D: Appl. Phys.* **44** 105104
[56] Schinca D C and Scaffardi L B 2008 *Nanotechnology* **19** 495712
[57] Prescott S W and Mulvaney P 2006 *J. Appl. Phys.* **99** 123504
[58] Johnson P B and Christy R W 1972 *Phys. Rev.* B **6** 4370–9
[59] Slaughter L S, Chang W-S, Swanglap P, Tcherniak A, Khanal B P, Zubarev E R and Link S 2010 *J. Phys. Chem.* C **114** 4934–8
[60] Bryant G W, Garcia de Abajo F J and Aizpurua J 2008 *Nano Lett.* **8** 631–6